Journal of Trace Elements in Medicine and Biology 90 (2025) 127694

Contents lists available at ScienceDirect

Journal of Trace Elements in Medicine and Biology

journal homepage: www.elsevier.com/locate/jtemb

Nerve growth factor acts as a modulator on the p38 MAPK pathway in copper-induced liver damage

Mustafa Usta [a,1,*], Yılmaz Çiğremiş [b,2], Hasan Özen [a,3]

[a] Department of Pathology, Faculty of Veterinary Medicine, Balıkesir University, Balıkesir 10100, Turkiye
[b] Departman of Medical Biology and Genetics, Faculty of Medicine, İnönü University, Malatya 44280, Turkiye

ARTICLE INFO

Keywords:
Copper
Hepatotoxicity
Nerve Growth Factor (NGF)
P38 MAPK
SB203580

ABSTRACT

Background: Copper (Cu) toxicity induces oxidative and nitrosative stress in hepatocytes, leading to inflammation and apoptosis. Nerve Growth Factor (NGF), known for its neuroprotective properties, may influence liver tissue via the p38 MAPK pathway; however, its role in Cu-induced hepatotoxicity remains unclear, and hence the aim of this study is to investigate the protective role of exogenous NGF in a Cu-induced liver injury model in mice, with a focus on p38 MAPK pathway.

Methods: Sixty-four adult male BALB/c mice were equally divided into eight groups, with each group receiving intraperitoneal injections 3 times at 24 h intervals of their respective substances at the following doses: 0.9 % NaCl (Control), 10 μg/kg NGF (NGF), 20 mg/kg SB203580 (p38MAPKi), 10 μg/kg NGF + 20 mg/kg SB203580 (NGF+p38MAPKi), 20 mg/kg $CuSO_4$ (Cu), 20 mg/kg $CuSO_4$ + 10 μg/kg NGF (Cu+NGF), 20 mg/kg $CuSO_4$ + 20 mg/kg SB203580 (Cu+p38MAPKi), and 20 mg/kg $CuSO_4$ + 10 μg/kg NGF + 20 mg/kg SB203580 (Cu+NGF+p38MAPKi). Liver tissues were analyzed using histopathological, immunohistochemical, biochemical, and molecular methods.

Results: $CuSO_4$ exposure caused severe hepatic damage, evidenced by hydropic degeneration, focal necrosis, and elevated apoptosis (Caspase 3 and 8). It also increased ALT/AST levels and oxidative/nitrosative stress markers (MDA, TOC, iNOS, nitrotyrosine), while reducing antioxidant markers (GSH, TAC). NGF administration significantly ameliorated these alterations, improved antioxidant status, and reduced pro-inflammatory cytokines (IL-1, IL-6, TNF-α). These effects were abrogated by co-treatment with SB203580, implicating p38 MAPK involvement.

Conclusion: NGF exerts hepatoprotective effects against Cu-induced toxicity by modulating oxidative stress, inflammation, and apoptosis through the p38 MAPK signaling pathway. These findings underscore NGF's potential as a therapeutic candidate for oxidative liver injuries.

1. Introduction

Copper (Cu) is a widely distributed metal on Earth, known for its ability to readily exchange electrons allowing to act as a catalyst in the electron transfer processes of enzymes involved in various biological functions [1]. Cu plays a critical role in cellular homeostasis by contributing to the structure and activity of enzymes such as copper-zinc superoxide dismutase, ceruloplasmin, ferroxidase, lysyl oxidase, tyrosinase, dopamine-β monooxygenase, copper amine oxidase, and hephaestin ferroxidase [2]. Cu metabolism in humans and animals is regulated through intestinal absorption, hepatic storage, and excretion of excess Cu via bile [3]. Under physiological conditions, Cu levels are tightly controlled by intracellular systems, but excessive accumulation may result in toxicity [4]. The liver, as the central organ for Cu metabolism, is particularly susceptible to Cu-induced toxicity. Studies suggest that elevated reactive oxygen (ROS) and nitrogen species (RNS) play a pivotal role in Cu-induced liver damage [5,6].

Nerve Growth Factor (NGF) is a founding member of the neurotrophin family, a group of extracellular molecules critical for the survival, growth, differentiation, and function of neurons [7]. Beyond its

* Corresponding author.
E-mail addresses: mustafa.usta@balikesir.edu.tr (M. Usta), yilmazcigremis@hotmail.com (Y. Çiğremiş), hasanozen@hotmail.com (H. Özen).
[1] ORCID ID: https://orcid.org/0000-0002-3346-9097
[2] ORCID ID: https://orcid.org/0000-0002-8600-0946
[3] ORCID ID: https://orcid.org/0000-0002-6820-2536

https://doi.org/10.1016/j.jtemb.2025.127694
Received 28 April 2025; Received in revised form 2 July 2025; Accepted 7 July 2025
Available online 8 July 2025

roles in nervous tissue, it is involved in various biological processes, including wound healing in skin and mucous membranes, corneal epithelial regeneration, regulation of intestinal motility and mucus secretion, and modulation of inflammatory responses through mast cells and basophils in the immune system [7,8]. NGF exerts its effects by binding to the TrkA receptor on the cell membrane, triggering tyrosine phosphorylation. This phosphorylation event activates adaptor proteins, which subsequently initiate intracellular signaling cascades and hence activate specific genes [9,10]. NGF by activating the Mitogen Activated Protein Kinase (MAPK) signaling pathway plays important roles in cellular metabolism [11].

MAPKs play essential roles in eukaryotic organisms, from yeast to humans, regulating fundamental processes such as cell proliferation, differentiation, and apoptosis [12]. Activated by growth factors, cytokines, and oxidative stress, MAPKs facilitate the cellular response to various stimuli. In mammals, MAPKs are categorized into three groups: extracellular signal-regulated kinases (ERK), c-Jun N-terminal kinases (JNK), and p38 MAPKs [13]. The p38 MAPK signaling pathway is particularly responsive to growth factors, environmental stressors, and inflammatory cytokines. NGF, as a growth factor, has been shown to activate this pathway [13,14]. However, the precise role of this interaction in modulating cell damage or cell survival remains unclear. Therefore, this study investigates the potential role of NGF in copper-induced liver injury in mice, with particular emphasis on the p38 MAPK pathway, using histopathological, biochemical, and molecular methods.

2. Material and methods

2.1. Animals and treatments

This study was carried out in 64 adult male BALB/c mice (weighing 30 ± 5 g) obtained from Balıkesir University Experimental Animal Production, Care, Application and Research Centre with the approval of Balıkesir University Animal Experiments Local Ethics Committee dated 24.02.2022 and numbered 2022/1–9. One week before the start of the study, the mice were placed in a room where the temperature was kept under control between 22°C and humidity between 60 % and 65 % and 12 h light (08:00–20:00) and 12 h dark cycle was applied. Mice were fed *ad libitum* with standard mouse chow and drank tap water. Mice were randomly and equally divided into eight groups, with each group receiving intraperitoneal injections (ip) of their respective substances at 24-hour intervals for a total of three injections. The administered doses were as follows: Control group: 0.9 % NaCl; NGF group: 10 μg/kg NGF (Mouse NGF, Catalogue No: 120a.a, MedChem Express); p38MAPKi group: 20 mg/kg p38 MAPK inhibitor (SB203580, Catalogue No: A10824, AdooQ Bioscience); NGF+p38MAPKi group: 10 μg/kg NGF and 20 mg/kg SB203580; Cu group: 20 mg/kg CuSO4 (Catalogue No: 7758–99–8, Merck); Cu+NGF group: 20 mg/kg CuSO4 and 10 μg/kg NGF; Cu+p38MAPKi group: 20 mg/kg CuSO4 and 20 mg/kg SB203580; Cu+NGF+p38MAPKi group: 20 mg/kg CuSO4, 10 μg/kg NGF, and 20 mg/kg SB203580.

2.2. Histopathology

Liver tissue samples from each animal were routinely fixed in %10 formaldehyde, embedded in paraffin, cut at 4.5 μm, stained with hematoxylin and eosin (HE), and observed under light microscope for histopathological changes. The histopathological score of each case was determined according to the zonal location of the lesions (degeneration and necrosis) and the number of Kupffer cells. The histopathological score criteria were degeneration; 0: none, 1: only in zone 3, 2: in the 2nd and 3rd zones, 3: in the 1st, 2nd and 3rd zones; necrosis 0: none, 1: only in zone 3, 2: in the 2nd and 3rd zones, 3: in the 1st, 2nd and 3rd zones; using Qupath (version, v0.4.3) digital pathology image analysis software, 5 different photographs taken at 200X magnification from each section were obtained according to the average number of Kupffer cells, 0: $\leq$ 30, 1: 31–40, 2: 41–50; 3: $\geq$ 51.

2.3. Immunohistochemistry (IHC)

Liver tissue sections cut from the paraffin blocks were stained by avidin-biotin-peroxidase method for iNOS (1/500, PA5–16855 İnvitrogen), Nitrotyrosine (1/500, Ab5411 Millipore), IL-1 (1/300, Bs-6319R Bioss), IL-6 (1/300, Bs-4539R Bioss), TNF-α (1/100, BT-AP15035 BT LAP), Caspase 3 (1/200, ab13847 Abcam) and Caspase 8 (1/200, ab4052 Abcam). For each antibody used in the study, a negative control was performed by applying PBS instead of the primary antibody. Immunoreactivity in the tissue samples was visualized by the help of diaminobenzidine/H_2O_2 treatment. The tissue samples were observed under a light microscope and representative photographs obtained by the help of digital camera integrated into the light microscope. Fiji (version 2.12.0) digital pathology image analysis software was used for image analysis. The ratio of immune positive areas to other areas in each photograph was calculated as a percentage. For each case and each antibody, 5 different images taken at 200X magnification were used and the average of the obtained percentages was accepted as the score for that subject and antibody.

2.4. Biochemical analyses

2.4.1. Blood serum

At the end of the study, blood samples were collected from the sacrificed mice and then centrifuged at 3000 rpm for 15 min to obtain serum. AST, ALT and GGT enzyme levels, which are markers of liver damage, were measured in serum samples using an autoanalyzer (Randox imola, Antrim). Data were presented as U/L.

2.4.2. Liver tissues

MDA levels in liver homogenates were detected according to the method of Mihara and Uchiyama and the results were presented as nanomoles of MDA per gram of wet tissue (nmol/gwt) [15].

GSH levels were measured using the method described by Ellman [16]. Reduced GSH were reacted with 5,5-dithiobis-2-nitrobenzoic acid and detected spectrophotometrically at 410 nm. The results were presented as nmol/gwt.

Liver tissue TAC (Catalogue No: MS22128A) and TOC (Catalogue No: MK221460) analyses were performed according to the instructions provided by Rel Assay Diagnostic company.

2.5. mRNA expression by qRT-PCR

RNA extraction from liver samples was done following the instructions of the RNA isolation kit (SanPrep Column MicroRNA Mini-Prep Kit, Catalogue No: SK8811, BIO BASIC). cDNA synthesis kit (OneScript Plus cDNA Synthesis Kit, Catalogue No: G236, abm) was used to synthesize cDNA in accordance with instructions provided by the manufacturer. cDNA sequences of p38 MAPK were taken from NCBI and, β-Actin was used as the reference gene. Sentebiolab (Ankara, Türkiye, Table 1) was entrusted to design and synthesize the primers. By using the SYBR® Green Master kit (BlasTag 2X qRT-PCR MasterMix, Catalog No: G891, abm), qRT-PCR was conducted by adopting a Rotor-Gene Q 5PLEXHRM real-time thermal cycler following standard protocols. The

Table 1
Primer sequences of genes selected for analysis by qRT-PCR.

Target gene	Primer Sequence (5'-3')	Tm(°C)
β-Actin-F	5'-CTGGCTCCTAGCACCATGA−3'	60.21
β-Actin-R	5'-TAGAGCCACCAATCCACACA−3'	55.68
p38 MAPK-F	5'-CCGGATCCTGGAAGATGTCGCAGGAGAG−3'	65.78
p38 MAPK-R	5'-CCGGATCCCCAGGTGCTCAGGACACCAT−3'	67.24

cycling protocol was as follow; initial denaturation at 95°C for 3 min, followed by 50 cycles of denaturation at 95°C for 15 sec, annealing at 60°C for 1 min, and extension at 60°C for 1 min. Each sample was run in triplicate. The qRT-PCR results were analyzed using the $2^{-\Delta\Delta CT}$ method [17].

2.6. Statistical analysis

The data obtained from histopathological, biochemical and molecular methods were statistically analyzed using GraphPad Prism 9.0 (Graphpad Software, La Jolla, California). All data belonging to the parameters investigated in the study showed normal distribution. Therefore, the data were analyzed by one-way ANOVA test and post-hoc Tukey HSD analysis was performed to determine the differences between the groups. The results were expressed as mean and standard error (X ± SE) and $P < 0.05$ was considered statistically significant.

3. Result

3.1. Histopathology

In histopathological examination, no pathological changes were observed in liver tissues of Control, NGF, p38MAPKi and NGF+p38MAPKi groups. In Cu, Cu+NGF, Cu+p38MAPKi, and Cu+NGF+p38MAPKi groups, degenerative changes ranging from hydropic degeneration to vacuolar degeneration and focal necrosis were detected in hepatocytes. Degenerated cells were generally larger and pale as compared to the healthy hepatocytes, and some had vacuoles of varying sizes in their cytoplasm. In addition to degeneration, necrosis of some hepatocytes was observed in these groups. Degeneration and necrosis were more prominent especially in hepatocytes in the centrilobular region, and these lesions extended to hepatocytes in the portal area in cases with severe damage (Table 2 and Fig. 1). The scores and statistical evaluation of histopathological findings according to the groups are shown in Fig. 2.

3.2. Immunohistochemistry (IHC)

Expression levels of NGF, iNOS, nitrotyrosine, Caspase 8, Caspase 3, IL-1, IL-6 and TNF-α in mouse liver tissues, immunohistochemical scores and statistical evaluation are shown in Fig. 2.

In Control, NGF, p38MAPKi and NGF+p38MAPKi groups, positive immunoreactivity of NGF was seen intracytoplasmic in a small number of hepatocytes (1–4 cells randomly distributed in each lobule). In Cu, Cu+NGF, Cu+p38MAPKi and Cu+NGF+p38MAPKi groups, NGF immunoreactivity was observed in hepatocytes with varying strong immunoreactivity from the central vein periphery to the portal area (Fig. 3).

iNOS immunoreactivity was observed in the cytoplasm of hepatocytes in the Control, NGF, p38MAPKi and NGF+p38MAPKi groups in a small number of hepatocytes around the central vein and randomly distributed in the lobule. In Cu and Cu+NGF+p38MAPKi groups, strong iNOS immunoreactivity was detected intracytoplasmic in hepatocytes between the central vein and portal area. In Cu+NGF and Cu+p38MAPKi groups, iNOS immunoreactivity was observed intracytoplasmic in hepatocytes ranging from the central vein to the portal area (Fig. 4).

Nitrotyrosine immunoreactivity was observed intracytoplasmic in a small number of hepatocytes in Control, NGF, p38MAPKi and NGF+p38MAPKi groups. In Cu and Cu+NGF+p38MAPKi groups, strong immunoreactivity was observed in hepatocytes between the central vein and portal area. Nitrotyrosine immunoreactivity was strong immunoreactivity around the central vein in Cu+NGF and Cu+p38MAPKi groups compared to the other Cu-treated groups (Fig. 5).

Caspase 8 immunoreactivity was seen intracytoplasmic in single hepatocytes randomly distributed in the lobule in Control, NGF, p38MAPKi and NGF+p38MAPKi groups. In Cu, Cu+p38MAPKi and

Table 2
Statistical averages of histopathological and immunohistochemical scoring of liver tissues findings by groups.

Group	Histopathology (X ± SE)	NGF (X ± SE)	iNOS (X ± SE)	Nitrotyrosine (X ± SE)	Caspase 8 (X ± SE)	Caspase 3 (X ± SE)	IL-1 (X ± SE)	IL-6 (X ± SE)	TNF-α (X ± SE)
Control	0.38 ± 0.183^{a}	3.97 ± 0.17^{a}	6.02 ± 0.55^{a}	4.06 ± 0.27^{a}	4.88 ± 0.32^{a}	4.18 ± 0.45^{a}	7.07 ± 0.51^{a}	4.03 ± 0.40^{a}	3.63 ± 0.20^{a}
NGF	0.63 ± 0.263^{a}	4.64 ± 0.36^{a}	7.32 ± 0.36^{a}	4.71 ± 0.40^{a}	4.41 ± 0.51^{a}	3.85 ± 0.29^{a}	13.66 ± 1.50^{a}	4.44 ± 0.48^{a}	3.70 ± 0.23^{a}
p38MAPKi	0.75 ± 0.250^{a}	4.39 ± 0.41^{a}	7.36 ± 0.36^{a}	5.81 ± 0.77^{a}	5.50 ± 0.48^{a}	4.61 ± 0.36^{a}	14.24 ± 1.48^{a}	4.55 ± 0.23^{a}	3.64 ± 0.17^{a}
NGF+p38MAPKi	0.50 ± 0.189^{a}	5.21 ± 0.53^{a}	7.60 ± 0.50^{a}	6.09 ± 0.44^{a}	5.26 ± 0.46^{a}	5.83 ± 0.73^{a}	15.00 ± 1.62^{a}	6.38 ± 0.41^{a}	4.01 ± 0.53^{a}
Cu	6.38 ± 0.263^{b}	38.04 ± 1.78^{b}	42.44 ± 2.01^{b}	34.80 ± 2.07^{b}	23.66 ± 1.62^{b}	20.66 ± 1.13^{b}	53.81 ± 3.75^{b}	45.41 ± 1.57^{b}	66.03 ± 2.08^{b}
Cu+NGF	4.13 ± 0.227^{c}	20.41 ± 1.81^{c}	18.09 ± 1.98^{c}	15.71 ± 0.77^{c}	13.69 ± 1.13^{c}	12.60 ± 0.75^{c}	31.01 ± 1.91^{c}	16.02 ± 0.95^{c}	56.77 ± 1.75^{c}
Cu+p38MAPKi	5.25 ± 0.250^{d}	29.28 ± 1.70^{d}	28.80 ± 2.17^{d}	23.89 ± 1.79^{d}	22.03 ± 1.18^{b}	18.17 ± 1.20^{b}	39.16 ± 1.62^{c}	30.92 ± 2.49^{d}	56.69 ± 2.06^{c}
Cu+NGF+p38MAPKi	5.38 ± 0.183^{d}	36.20 ± 1.79^{b}	35.87 ± 1.50^{e}	44.23 ± 2.33^{e}	26.36 ± 1.55^{b}	22.16 ± 1.67^{b}	49.52 ± 1.78^{b}	38.26 ± 2.87^{e}	67.90 ± 3.58^{b}

The data represent the histopathology score and percentage of immunoreactive area and are presented as mean ± standard error (X ± SE). Comparisons were made using one-way ANOVA followed by post-hoc Tukey HSD test. Different superscripts within the same column indicate a statistically significant difference between groups ($P < 0.05$).

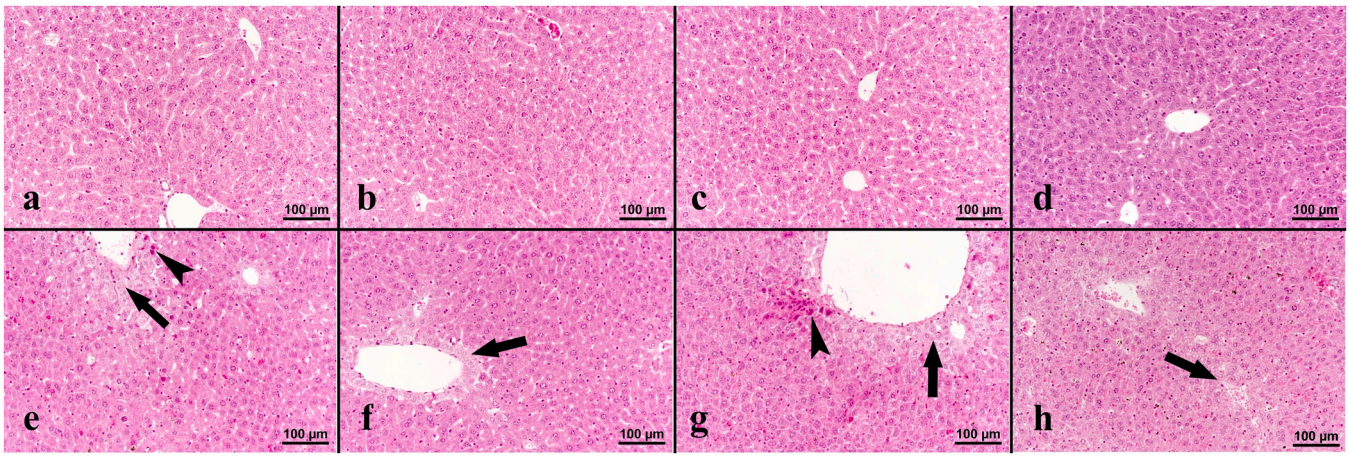

Fig. 1. Histopathological view of liver tissue: **a.** Control group, **b.** NGF group, **c.** p38MAPKi group, **d.** NGF+p38MAPKi group, **e.** Cu group, **f.** Cu+NGF group, **g.** Cu+p38MAPKi group, **h.** Cu+NGF+p38MAPKi group. While the liver tissue of non-Cu-treated groups appears histomorphologically normal, hydropic degeneration (arrow) and hepatocellular necrosis (arrow head) are evident in Cu-treated groups. HE.

Cu+NGF+p38MAPKi groups, Caspase 8 immunoreactivity was detected in hepatocytes located from the central vein to the portal area. In Cu+NGF group, immunoreactivity limited to hepatocytes around the central vein was observed (Fig. 6).

In Control, NGF, p38MAPKi and NGF+p38MAPKi groups, Caspase 3 immunoreactivity was observed intracytoplasmic in few hepatocytes within the lobule. In Cu, Cu+p38MAPKi and Cu+NGF+p38MAPKi groups, Caspase 3 immunoreactivity was especially strong in hepatocytes around the central vein and randomly distributed weak immunoreactivity was detected in hepatocytes in other areas of the lobule. In Cu+NGF group, Caspase 3 immunoreactivity was observed only in hepatocytes around the central vein (Fig. 7).

In the control group, IL-1 immunoreactivity was observed only in hepatocytes around the central vein with weak immunoreactivity. In NGF, p38MAPKi and NGF+p38MAPKi groups, IL-1 immunoreactivity was found to be moderate in hepatocytes around the central vein and decreased gradually towards the portal area. In Cu, Cu+p38MAPKi and Cu+NGF+p38MAPKi groups, IL-1 immunoreactivity was observed intracytoplasmic in all hepatocytes with decreasing strongly especially from the central vein to the portal area. In Cu+NGF group, IL-1 immunoreactivity was observed only in hepatocytes around the central vein with moderate, while the strongly of the reaction decreased towards the portal area (Fig. 8).

IL-6 immunoreactivity was present in the cytoplasm of a small number of hepatocytes randomly distributed in the lobule in Control, NGF, p38MAPKi and NGF+p38MAPKi groups. In Cu, Cu+p38MAPKi and Cu+NGF+p38MAPKi groups, strong IL-6 immunoreactivity was detected strongly immunoreactivity in hepatocytes around the central vein. In Cu+NGF group, IL-6 immunoreactivity was observed in hepatocytes around the central vein (Fig. 9).

In control, NGF, p38MAPKi and NGF+p38MAPKi groups, mild and intracytoplasmic TNF-α immunoreactivity was observed in hepatocytes around the central vein. In Cu, Cu+NGF, Cu+p38MAPKi and Cu+NGF+p38MAPKi groups, TNF-α immunoreactivity was detected strong immunoreactivity in hepatocytes around the central vein. No TNF-α immunoreactivity was observed in hepatocytes close to the portal area in these groups (Fig. 10).

3.3. Changes in the p38 MAPK expressions level

p38 MAPK expression levels in liver tissues are shown in Table 3 and Fig. 11. p38 MAPK expression was significantly ($P < 0.05$) higher in the Cu group than that of in the Control group. No significant difference was detected between the Control and p38MAPKi groups ($P > 0.05$). Compared to these two groups, p38 MAPK expressions in NGF and NGF+p38MAPKi groups were significantly ($P < 0.05$) higher. It was observed that p38 MAPK expression increased in Cu+p38MAPKi group compared to the control group, but it was not significantly different from that of the Cu group ($P > 0.05$). Similarly, the difference in p38 MAPK expression between Cu+NGF+p38MAPKi and Cu+NGF groups was not significant ($P > 0.05$).

3.4. Biochemical analysis

The results of all biochemical analyses are shown in Fig. 11. Serum ALT level was significantly increased ($P < 0.05$) in the Cu group compared to the other groups. The level in Cu+NGF group was significantly decreased ($P < 0.05$) compared to Cu+p38MAPKi and Cu+NGF+p38MAPKi groups. In Control, NGF, p38MAPKi, NGF+p38MAPKi groups, serum ALT levels were similar to each other ($P > 0.05$). There was no difference between Cu+p38MAPKi and Cu+NGF+p38MAPKi groups ($P > 0.05$). Serum AST level was significantly increased ($P < 0.05$) in the Cu and Cu+NGF+p38MAPKi groups compared to the other groups. A significant decrease ($P < 0.05$) in serum AST level was detected in the Cu+NGF group compared to the Cu group but still were significantly higher than that of the Control group ($P < 0.05$). No significant change was observed in serum GGT level among the groups in this study ($P > 0.05$). A significant increase in liver MDA level was seen in Cu group compared to the other groups ($P < 0.05$). The differences in liver MDA levels between Control, NGF, p38MAPKi, NGF+p38MAPKi, Cu+ NGF, Cu+p38MAPKi groups were not significant ($P > 0.05$). Liver GSH activity was detected to decrease significantly in Cu, Cu+p38MAPKi and Cu+NGF+p38MAPKi groups compared to Control, NGF, p38MAPKi, NGF+p38MAPKi and Cu+NGF groups ($P < 0.05$). Liver TOC level significantly increased in the Cu group as compared to the other groups ($P < 0.05$). The liver TOC levels did not differ significantly among the groups ($P < 0.05$). Liver TAC activity was noted to decrease significantly in Cu, Cu+p38MAPKi and Cu+NGF+p38MAPKi groups compared to Control, NGF, p38MAPKi, NGF+p38MAPKi and Cu+NGF groups ($P < 0.05$).

4. Discussion

Cu is a fundamental micronutrient and a vital catalytic cofactor in numerous biological processes, including mitochondrial respiration, antioxidant defense, and protein synthesis [5,18]. In mammals, dietary Cu is absorbed through intestinal epithelial cells and transported to the liver via the portal circulation. The liver acts as the main Cu reservoir in the body, regulating its distribution to peripheral organs via the bloodstream or its excretion through the bile [5,19]. These mechanisms

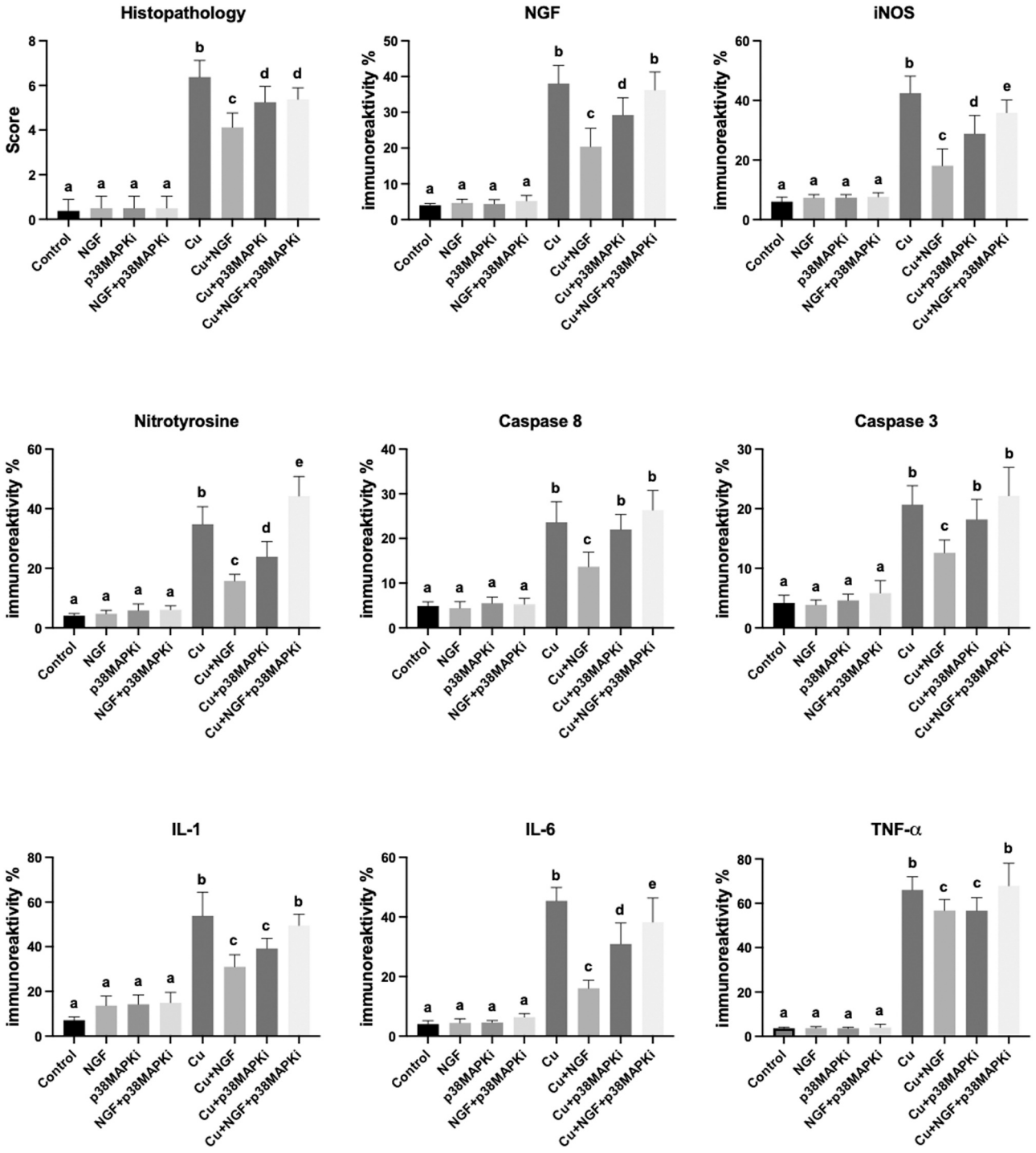

Fig. 2. Histopathological scoring of liver findings and expression levels of NGF, iNOS, nitrotyrosine, Caspase 8, Caspase 3, IL-1, IL-6, and TNF-α in mouse liver tissues, assessed through immunohistochemical analysis and statistical evaluation. Data are presented as mean ± standard deviation and analyzed using one-way ANOVA followed by Tukey's HSD post-hoc test. Columns with different superscripts indicate statistically significant differences among groups ($P < 0.05$).

help maintain Cu homeostasis at both systemic and cellular levels. An increase in free Cu levels within cells leads to cytotoxicity associated with oxidative stress [18]. In the current investigation, significant increases were observed in the levels of ROS and RNS biomarkers, such as TOC, iNOS, nitrotyrosine, and MDA, while significant TAC and GSH levels decreased significantly in the group given only Cu. Additionally, consistent with the oxidative and nitrosative stress markers, the severity of histopathological findings and the levels of liver damage biomarkers, ALT and AST, were significantly increased in the Cu group. When these findings are evaluated together, it was determined that ip administration of 20 mg/kg $CuSO_4$ for 3 days in mice induces hepatocyte damage associated with oxidative stress.

NGF expression may increase in hepatocytes due to oxidative stress in humans [20], rats [21], and mice [22]. While NGF is widely recognized as a key growth factor in neuronal development and survival, studies also report elevated hepatic expression in response to diverse forms of liver injury [23,24]. However, the specific roles of NGF in hepatocytes are not yet fully understood, and its expression appears to vary depending on the experimental model and conditions. It has been shown that NGF protects mice liver against oxidative stress and xenobiotic

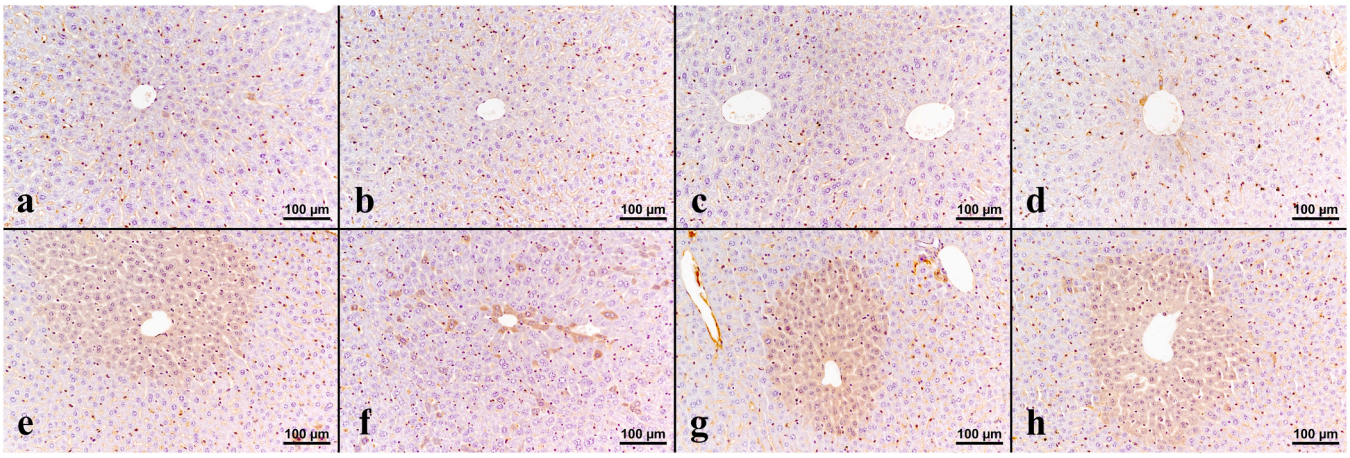

Fig. 3. NGF immunoreactivity in liver tissue: **a.** Control group, **b.** NGF group, **c.** p38MAPKi group, **d.** NGF+p38MAPKi group, **e.** Cu group, **f.** Cu+NGF group, **g.** Cu+p38MAPKi group, **h.** Cu+NGF+p38MAPKi group. Increased NGF immunoreactivity was generally observed in groups given to Cu compared to ungiven groups, with strong immunoreactivity in hepatocytes in close proximately around the central vein. Notably, NGF immunoreactivity in the Cu+NGF group was lower compared to the other Cu given groups. IHC.

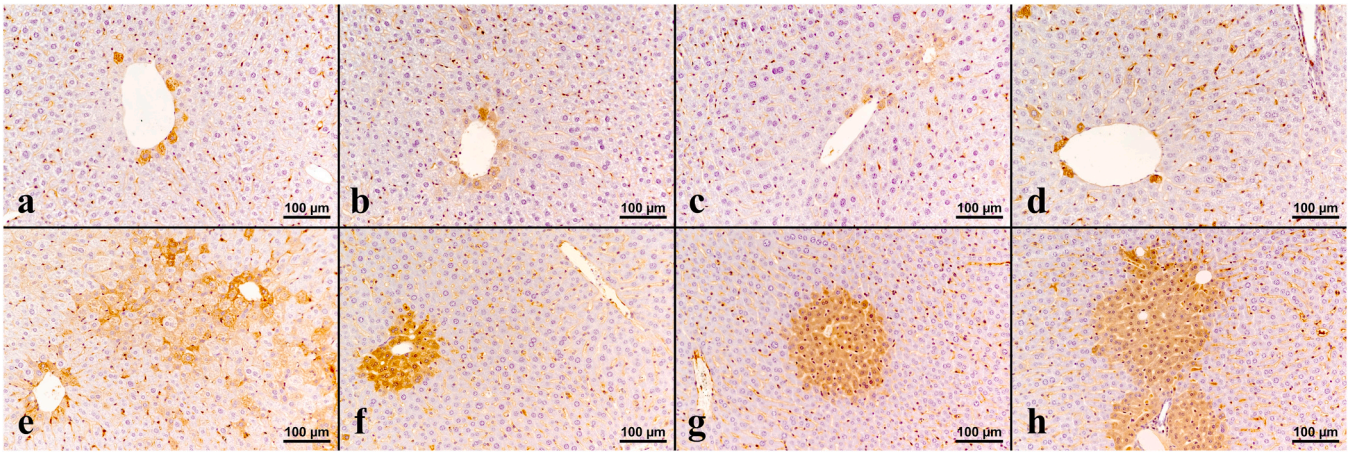

Fig. 4. iNOS immunoreactivity in liver tissue: **a.** Control group, **b.** NGF group, **c.** p38MAPKi group, **d.** NGF+p38MAPKi group, **e.** Cu group, **f.** Cu+NGF group, **g.** Cu+p38MAPKi group, **h.** Cu+NGF+p38MAPKi group. iNOS immunoreactivity was generally observed to be stronger in groups given to Cu compared to ungiven groups, with strong immunoreactivity hepatocytes in close proximately around the central vein. Notably, iNOS immunoreactivity in the Cu+NGF group appeared lower compared to other Cu given groups. IHC.

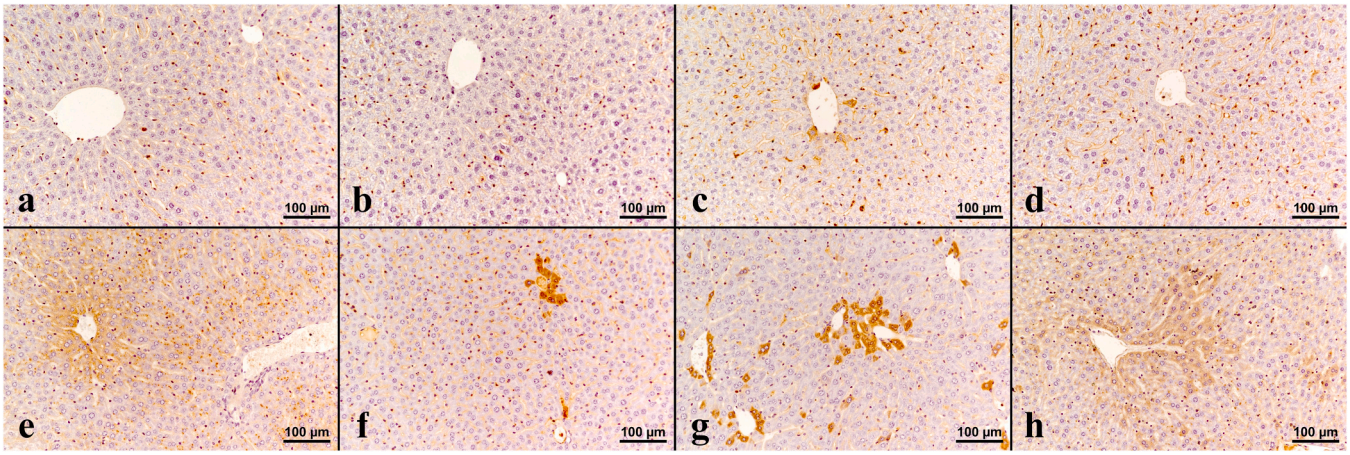

Fig. 5. Nitrotyrosine immunoreactivity in liver tissue: **a.** Control group, **b.** NGF group, **c.** p38MAPKi group, **d.** NGF+p38MAPKi group, **e.** Cu group, **f.** Cu+NGF group, **g.** Cu+p38MAPKi group, **h.** Cu+NGF+p38MAPKi group. Nitrotyrosine immunoreactivity was generally higher in groups given to Cu compared to ungiven groups, with strong immunoreactivity observed around hepatocytes in close proximately around the central vein. Notably, nitrotyrosine immunoreactivity in the Cu+NGF group appeared lower compared to other Cu given groups. IHC.

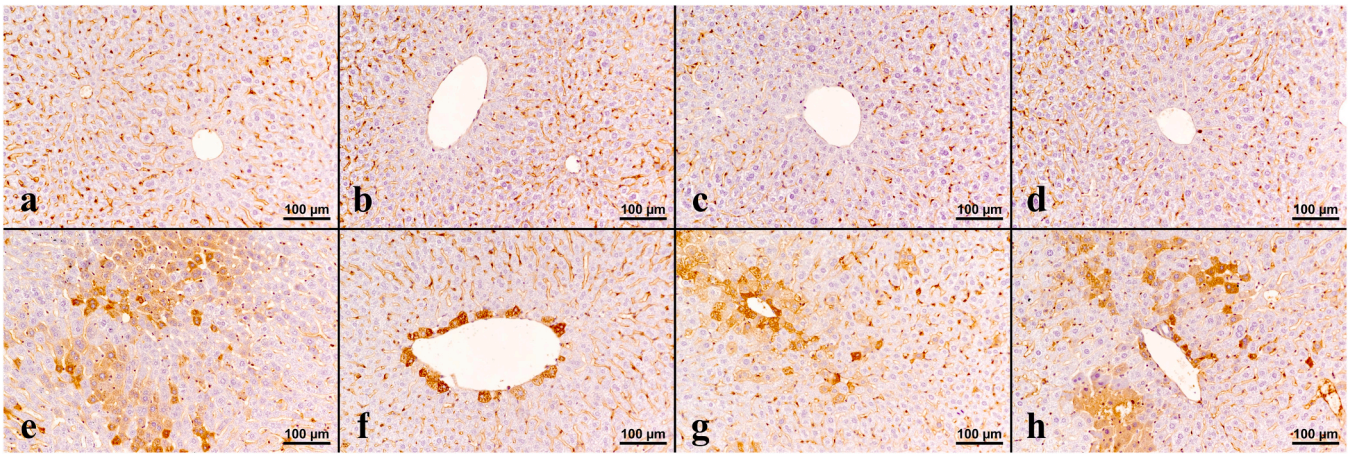

Fig. 6. Caspase 8 immunoreactivity in liver tissue: **a.** Control group, **b.** NGF group, **c.** p38MAPKi group, **d.** NGF+p38MAPKi group, **e.** Cu group, **f.** Cu+NGF group, **g.** Cu+p38MAPKi group, **h.** Cu+NGF+p38MAPKi group. Caspase 8 immunoreactivity was generally higher in groups given to Cu compared to ungiven groups, with strong immunoreactivity observed in close proximately around the central vein. Notably, Caspase 8 immunoreactivity in the Cu+NGF group appeared lower compared to other Cu given groups. IHC.

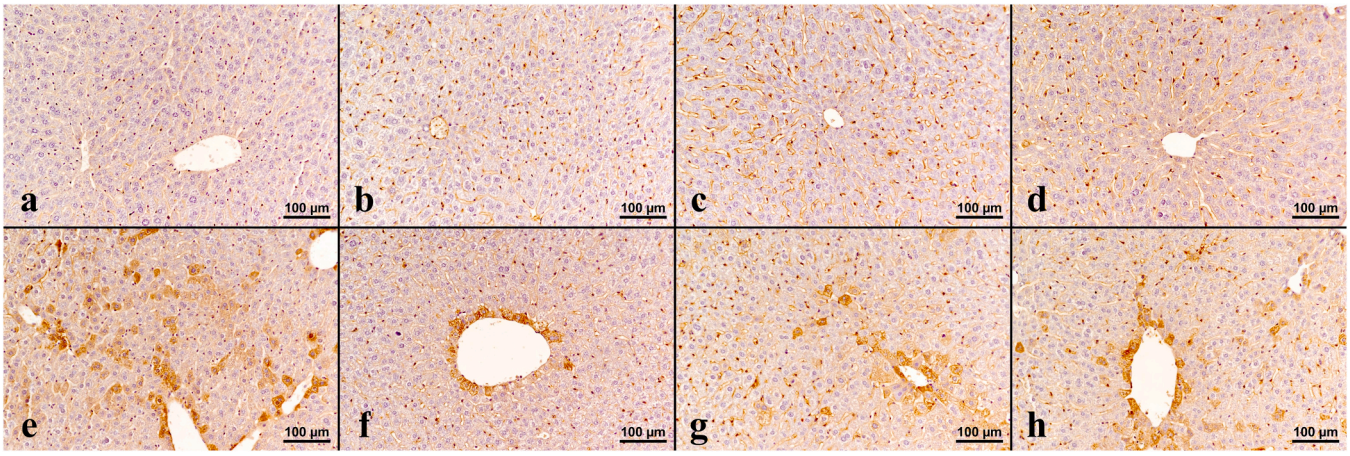

Fig. 7. Caspase 3 immunoreactivity in liver tissue: **a.** Control group, **b.** NGF group, **c.** p38MAPKi group, **d.** NGF+p38MAPKi group, **e.** Cu group, **f.** Cu+NGF group, **g.** Cu+p38MAPKi group, **h.** Cu+NGF+p38MAPKi group. Caspase 3 immunoreactivity was generally higher in groups given to Cu compared to ungiven groups, with strong immunoreactivity observed in close proximately around the central vein. Notably, Caspase 3 immunoreactivity in the Cu+NGF group appeared lower compared to other Cu given groups. IHC.

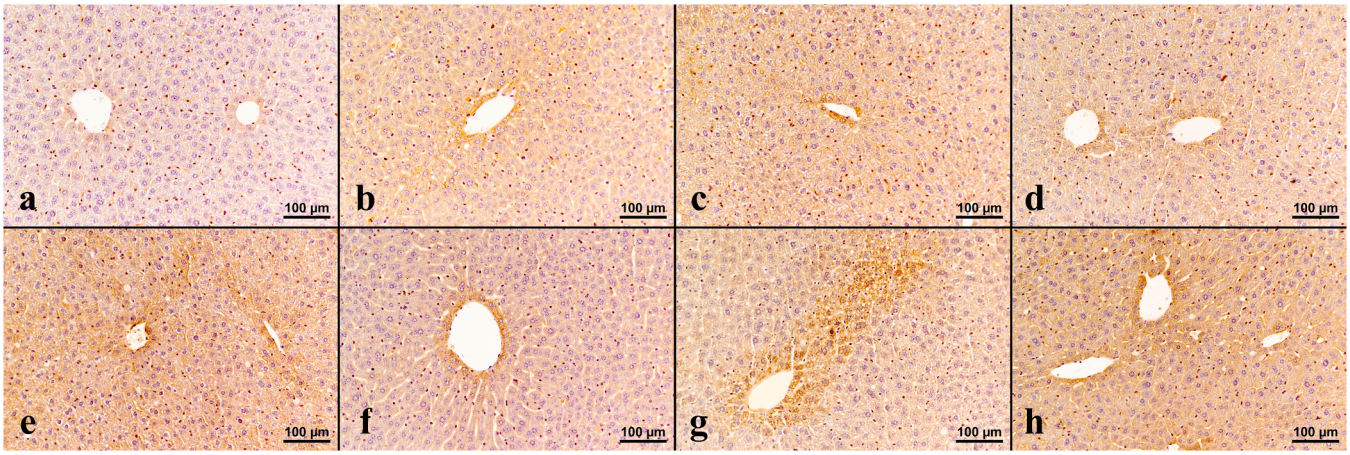

Fig. 8. IL-1 immunoreactivity in liver tissue: **a.** Control group, **b.** NGF group, **c.** p38MAPKi group, **d.** NGF+p38MAPKi group, **e.** Cu group, **f.** Cu+NGF group, **g.** Cu+p38MAPKi group, **h.** Cu+NGF+p38MAPKi group. IL-1 immunoreactivity was generally higher in groups given to Cu compared to ungiven groups, with strong immunoreactivity observed hepatocytes in close proximately around central vein. Notably, IL-1 immunoreactivity in the Cu+NGF group appeared lower compared to other Cu given groups. IHC.

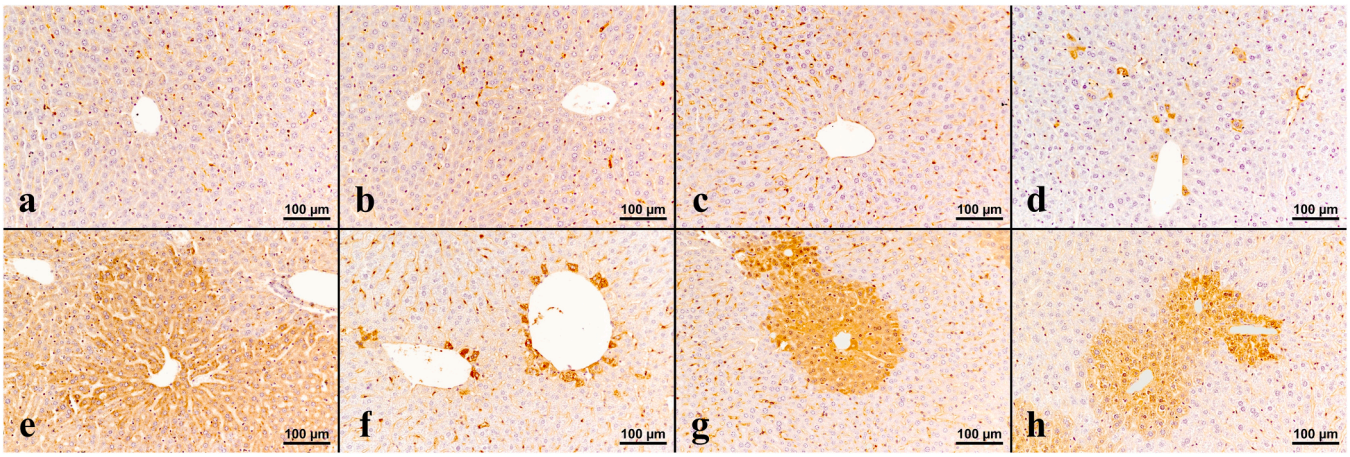

Fig. 9. IL-6 immunoreactivity in liver tissue: **a.** Control group, **b.** NGF group, **c.** p38MAPKi group, **d.** NGF+p38MAPKi group, **e.** Cu group, **f.** Cu+NGF group, **g.** Cu+p38MAPKi group, **h.** Cu+NGF+p38MAPKi group. IL-6 immunoreactivity was generally higher in groups given to Cu compared to ungiven groups, with strong immunoreactivity observed hepatocytes in close proximately around the central vein. Notably, IL-6 immunoreactivity in the Cu+NGF group appeared lower compared to other Cu given groups. IHC.

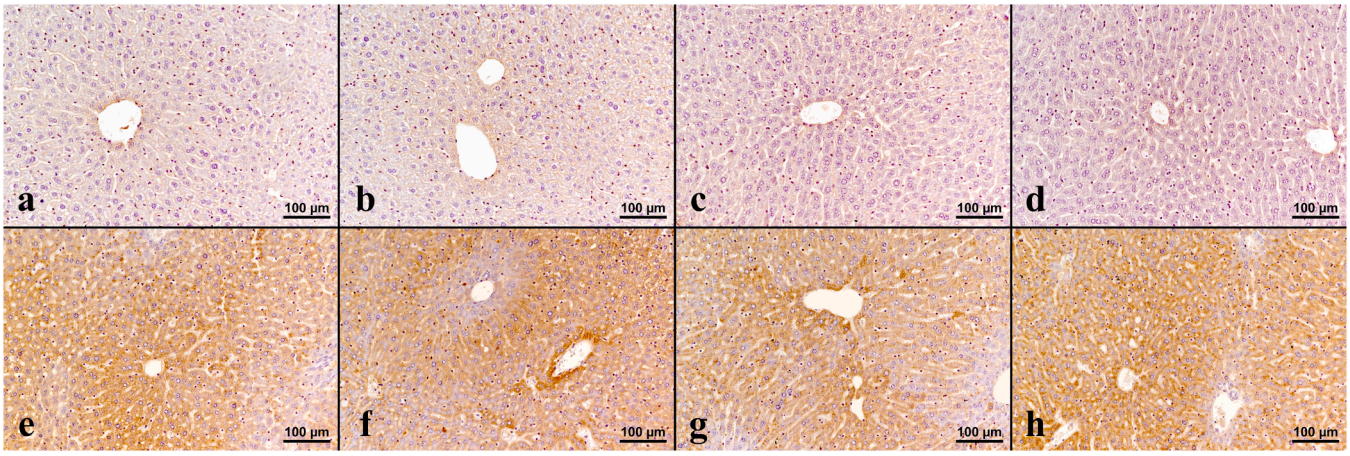

Fig. 10. TNF-α immunoreactivity in liver tissue: **a.** Control group, **b.** NGF group, **c.** p38MAPKi group, **d.** NGF+p38MAPKi group, **e.** Cu group, **f.** Cu+NGF group, **g.** Cu+p38MAPKi group, **h.** Cu+NGF+p38MAPKi group. TNF-α immunoreactivity was generally higher in groups given to Cu compared to ungiven groups, with strong immunoreactivity observed hepatocytes in close proximately around the central vein. IHC.

Table 3
Statistical data of hepatic p38 MAPK mRNA expression levels and biochemical analysis results by groups.

Group	***p38 MAPK* mRNA** X ± SE	**ALT** (U/L) X ± SE	**AST** (U/L) X ± SE	**GGT** (U/L) X ± SE	**TOC** µmol/L X ± SE	**TAC** µmol/L X ± SE	**GSH** nmol/gr X ± SE	**MDA** nmol/gr X ± SE
Control	0.47 ± 0.08^{a}	23.00 ± 1.33^{a}	105.13 ± 3.96^{a}	1.57 ± 0.21	37.79 ± 0.81^{a}	10.97 ± 0.24^{a}	2774.04 ± 257.42^{a}	80.09 ± 3.77^{a}
NGF	1.31 ± 0.09^{b}	25.13 ± 1.31^{a}	91.62 ± 4.29^{a}	3.30 ± 0.71	36.90 ± 0.14^{a}	10.20 ± 0.50^{a}	2823.94 ± 267.04^{a}	80.04 ± 5.70^{a}
p38MAPKi	0.41 ± 0.06^{a}	23.13 ± 0.81^{a}	95.00 ± 6.69^{a}	2.93 ± 0.74	37.31 ± 1.76^{a}	11.41 ± 0.37^{a}	3130.71 ± 138.09^{a}	83.81 ± 3.3^{a}
NGF+p38MAPKi	1.09 ± 0.08^{b}	26.38 ± 1.19^{a}	86.88 ± 6.54^{a}	2.70 ± 0.65	36.24 ± 0.78^{a}	9.48 ± 0.52^{a}	2978.40 ± 55.05^{a}	85.33 ± 3.44^{a}
Cu	1.45 ± 0.15^{bc}	147.87 ± 12.44^{b}	574.63 ± 37.67^{b}	4.15 ± 0.95	51.10 ± 0.64^{b}	6.30 ± 0.30^{b}	1324.17 ± 87.24^{b}	158.87 ± 11.94^{b}
Cu+NGF	1.83 ± 0.14^{c}	32.75 ± 2.25^{a}	311.50 ± 40.19^{c}	3.18 ± 0.80	36.55 ± 0.92^{a}	10.72 ± 0.45^{a}	2197.32 ± 218.84^{a}	106.06 ± 3.46^{ac}
Cu+p38MAPKi	1.39 ± 0.07^{bc}	97.88 ± 8.87^{c}	434.00 ± 46.34^{d}	4.47 ± 0.92	39.84 ± 0.55^{a}	4.40 ± 0.62^{b}	1147.54 ± 46.85^{b}	103.92 ± 7.62^{ac}
Cu+NGF+p38MAPKi	1.48 ± 0.11^{bc}	117.87 ± 6.58^{c}	466.13 ± 27.75^{b}	4.75 ± 1.10	43.43 ± 0.62^{a}	8.01 ± 0.37^{b}	1646.63 ± 120.22^{b}	126.26 ± 10.62^{c}

The data are presented as mean ± standard error (X ± SE) and were analyzed using one-way ANOVA followed by post-hoc Tukey HSD test. Different superscripts within the same column indicate statistically significant differences between groups ($P < 0.05$).

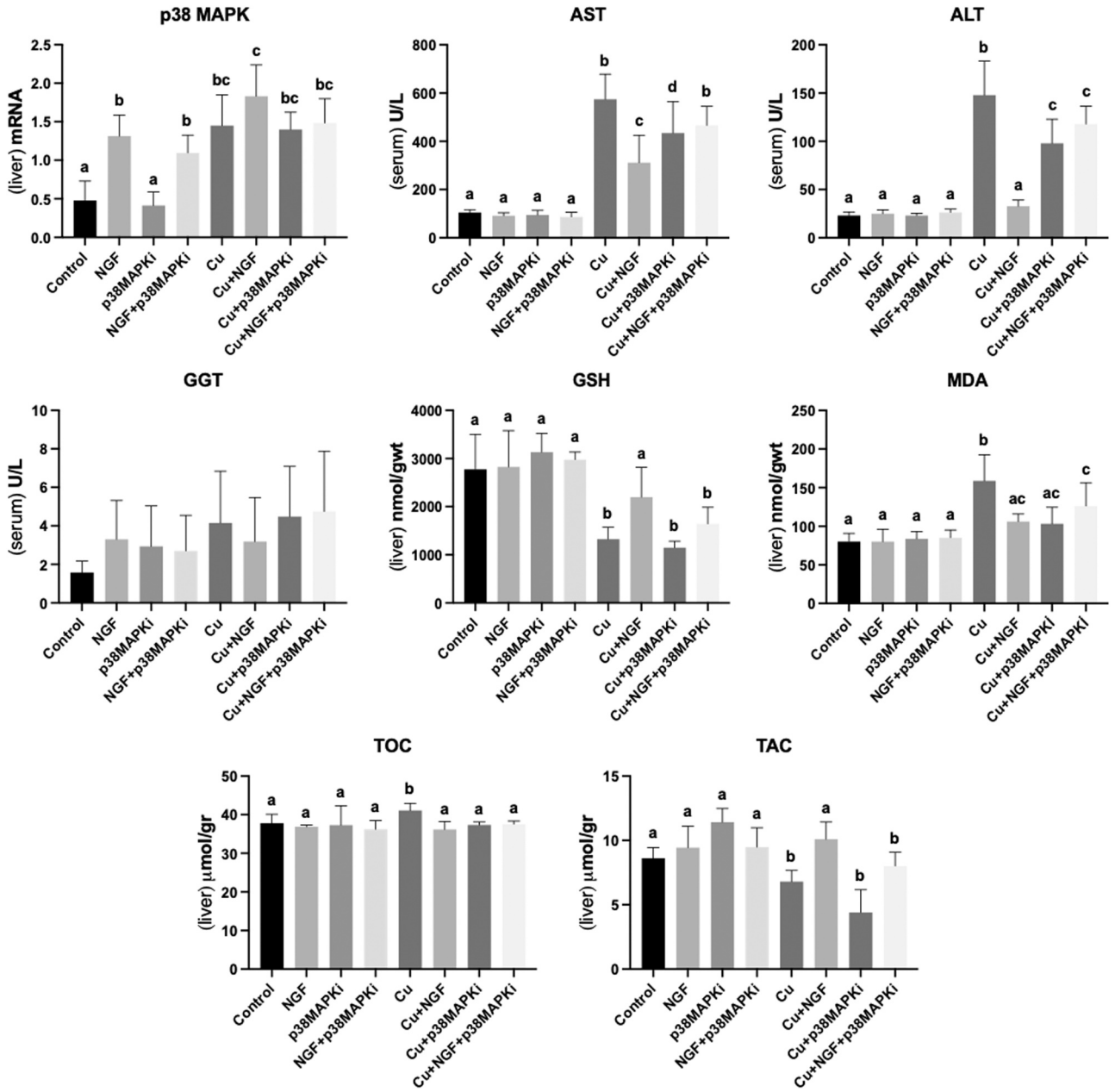

Fig. 11. mRNA expression levels of p38 MAPK and biochemical parameters (ALT, AST, TOC, TAC, GSH, and MDA) across groups, with significant differences observed ($P < 0.05$), except for GGT ($P > 0.05$). Data are expressed as mean ± standard deviation and analyzed using one-way ANOVA followed by Tukey's HSD post-hoc test. Columns with different superscripts indicate statistically significant differences among groups ($P < 0.05$).

damage caused by buthionine sulfoximine, arsenic, and acetaminophen [24]. It has also been detected that NGF is expressed by hepatocytes in response to oxidative stress caused by gallstones in humans and that NGF protects hepatocytes through the sirtuin 1 signaling pathway [20]. In CCl_4-induced liver injury, NGF has been reported to be expressed by hepatocytes, and this induces apoptosis in hepatic stellate cells via Caspase 3 activation [23]. In the present study, Cu-induced liver injury significantly increased NGF expression in hepatocytes. Interestingly, this was reflected by a significantly lower NGF immunoreactivity score in the Cu+NGF group compared to the Cu group ($P < 0.05$), suggesting a feedback suppression due to exogenous NGF supplementation. NGF exerts protective and regenerative effects in the liver by reducing oxidative stress, suppressing inflammation and improving liver function. These effects are mediated by regulating antioxidant metabolism, modulating stress response proteins and reducing ROS [25,26]. In the Cu+NGF group, MDA, TOC, iNOS, and nitrotyrosine levels were significantly lower, while GSH and TAC levels were significantly higher compared to the Cu group. Additionally, histopathological damage, as well as ALT and AST levels, were significantly lower in the Cu+NGF group compared to the Cu group. The increase in NGF expression in the Cu group is considered a cellular response to prevent oxidative damage, and the exogenously administered NGF is suggested to reduce oxidative stress, thereby leading to a lower amount of NGF expression from hepatocytes.

p38 MAPK, a member of the mitogen-activated protein kinase family, becomes activated in response to oxidative stress, growth factors, cytokines, and various other stimuli. There are hundreds of substrates within the cell to which active p38 MAPK can bind [12]. These substrates are involved in fundamental cellular processes such as cell proliferation, differentiation, survival, apoptosis, inflammation, and tissue homeostasis [12,27]. It has been reported that p38 MAPK expression increases in liver damage induced by Cu in mice [28]. Furthermore,

numerous studies have shown that stimulation of different cells with NGF leads to increased p38 MAPK expression [11,14,29,30]. In this study, p38 MAPK expression levels in the Cu and NGF groups were also significantly higher compared to the Control group. Most of the knowledge about p38 MAPK substrates comes from studies using chemical inhibitors like SB203580 [31–33]. SB203580, an imidazole group derivative, was initially known as a molecule suppressing cytokine production but was later identified as an inhibitor of p38 MAPK [13,34]. In this study, it was observed that the application of SB203580 as a p38 MAPK inhibitor did not have a detectable effect on p38 MAPK expression. It is stated that the inhibition of p38 MAPK by SB203580 is not due to its effect on the expression of this molecule but rather through its binding to p38 MAPK and blocking the functions of its substrates [11, 35]. It was observed that GSH and TAC levels in the Cu+NGF+p38-MAPKi group were significantly lower, while iNOS and nitrotyrosine levels were significantly higher compared to the Cu+NGF group. Additionally, ALT and AST levels, as well as the severity of histopathological lesions in the Cu+NGF+p38MAPKi group, were significantly higher than those in the Cu+NGF group. Activation of p38 MAPK within the cell enhances the expression of transcription factors and antioxidant enzymes, leading to a reduction in ROS and RNS levels and the activation of cellular repair mechanisms [36–38]. When these findings are evaluated together, we determined that NGF protects hepatocytes from oxidative stress through the p38 MAPK signaling pathway.

Oxidative stress resulting from Cu toxicity has been shown to elevate p38 MAPK expression in cells [39]. Activated by oxidative stress, p38 MAPK regulates cytokine expression downstream via Nuclear Factor kappa B (NF-κB) [40–42]. In liver damage induced by Cu in mice, NF-κB has been reported to induce the expression of IL-1, IL-6, and TNF-α [43]. In the present study, the expressions of IL-1, IL-6, and TNF-α in the Cu+NGF group were also observed to be significantly lower ($P < 0.05$) compared to the Cu group. NGF is known to regulate the expression of both anti-inflammatory and pro-inflammatory cytokines [44]. The lower levels of IL-1, IL-6, and TNF-α expressions in subjects treated with Cu and NGF compared to those treated with Cu alone were interpreted as demonstrating the anti-inflammatory effect of NGF. SB203580, a p38 MAPK inhibitor, is also known to have an inhibitory effect on pro-inflammatory cytokines. It has been reported that the inhibition of p38 MAPK leads to reduced expressions of IL-1, IL-6, and TNF-α in various toxicity models [32,45]. The expressions of IL-1, IL-6, and TNF-α in the Cu+NGF group were significantly lower compared to the Cu+NGF+p38MAPKi group. This finding suggests that NGF exerts its anti-inflammatory effect via the p38 MAPK pathway.

Oxidative stress caused by Cu has been reported to induce apoptosis in cells [46]. Excess Cu may also increase the expressions of Caspase 8 and Caspase 3 in tissues and cells other than the liver [47–49]. Increased levels of Caspase 8 and Caspase 3 expressions in the Cu-treated groups were detected compared to the groups without Cu treatment ($P < 0.05$). The expressions of Caspase 8 and Caspase 3 in the Cu+NGF group were significantly lower ($P < 0.05$) compared to the Cu group, which was thought to be due to the reduction of oxidative stress by NGF. Moreover, studies investigating its effects on tissues and cells other than the liver have reported that NGF increases the expression of anti-apoptotic molecules in mesenchymal stem cells [50], cerebral neurons [51], and bone marrow stem cells [52], thereby making these cells more resistant to apoptosis. Therefore, it was hypothesized in the current study that NGF might have protected hepatocytes from apoptosis by increasing the expression of anti-apoptotic molecules. While the expressions of Caspase 8 and Caspase 3 increased in subjects treated only with Cu, a significant decrease ($P < 0.05$) in the expressions of these molecules was observed when Cu was combined with NGF. Additionally, the expressions of Caspase 8 and Caspase 3 in the Cu+NGF group were significantly lower ($P < 0.05$) compared to the Cu+NGF+p38MAPKi group. These findings suggest that NGF exerts its anti-apoptotic effect on hepatocytes in Cu toxicity via the p38 MAPK signaling pathway.

5. Conclusion

The data of the current study indicated that 20 mg/kg ip $CuSO_4$ for three days caused prominent liver damage as shown by increases in the levels of ALT, AST, MDA, TOC, iNOS, and nitrotyrosine and decreases in GSH and TAC levels as well as histopathological changes. Simultaneous ip administration of 10 μg/kg NGF with Cu caused significant changes in these biomarkers, promoting cellular homeostasis. Additionally, exogenous NGF administration significantly reduced the expression of pro-inflammatory cytokines (IL-1, IL-6, and TNF-α) and apoptosis (Caspase 8 and Caspase 3) in hepatocytes. When the p38 MAPK inhibitor SB203580 was administered at a dose of 20 mg/kg along with Cu and NGF, the effects of NGF in cellular homeostasis and survival were diminished. All data indicates that p38 MAPK is a central modulator in cellular signaling and NGF plays an important role through this pathway in liver induced Cu damage.

CRediT authorship contribution statement

Yılmaz Çiğremiş: Methodology, Formal analysis. **Hasan Özen:** Writing – review & editing, Supervision, Project administration, Methodology, Investigation, Data curation, Conceptualization. **Mustafa Usta:** Writing – review & editing, Writing – original draft, Visualization, Methodology, Investigation, Data curation, Conceptualization.

Funding

This study was financed and supported by the Balıkesir University Scientific Research Co-ordinatorship (BAP Project No: 2022/038).

Declaration of Competing Interest

The authors declare that they have no known competing financial interests or personal relationships that could have appeared to influence the work reported in this paper.

Acknowledgments

We would like to express our gratitude to Musa Karaman and Fatma İlhan for important scientific suggestions and to Celalettin Çevik for technical support.

Appendix A. Supporting information

Supplementary data associated with this article can be found in the online version at doi:10.1016/j.jtemb.2025.127694.

References

[1] W. Kaim, J. Rall, Copper—a "Modern" bioelement, Angew. Chem. Int. Ed. Engl. 35 (1996) 43–60, https://doi.org/10.1002/anie.199600431.
[2] I. Scheiber, R. Dringen, J.F.B. Mercer, Copper: effects of deficiency and overload, in: A. Sigel, H. Sigel, R.K.O. Sigel (Eds.), Interrelations between Essential Metal Ions and Human Diseases, Springer Netherlands, Dordrecht, 2013, pp. 359–387, https://doi.org/10.1007/978-94-007-7500-8_11.
[3] M.C. Linder, Biochemistry of Copper, Springer US: Imprint, Springer, Boston, MA, 1991.
[4] V. Kumar, J. Kalita, H.K. Bora, U.K. Misra, Temporal kinetics of organ damage in copper toxicity: a histopathological correlation in rat model, Regul. Toxicol. Pharmacol. 81 (2016) 372–380, https://doi.org/10.1016/j.yrtph.2016.09.025.
[5] L. Gaetke, Copper toxicity, oxidative stress, and antioxidant nutrients, Toxicology 189 (2003) 147–163, https://doi.org/10.1016/S0300-483X(03)00159-8.
[6] H. He, Z. Zou, B. Wang, G. Xu, C. Chen, X. Qin, C. Yu, J. Zhang, Copper oxide nanoparticles induce oxidative DNA damage and cell death via copper ion-mediated P38 MAPK activation in vascular endothelial cells, IJN 15 (2020) 3291–3302, https://doi.org/10.2147/IJN.S241157.
[7] G. Dechant, H. Neumann, Neurotrophins, in: C. Alzheimer (Ed.), Molecular and Cellular Biology of Neuroprotection in the CNS, Springer US, Boston, MA, 2003, pp. 303–334, https://doi.org/10.1007/978-1-4615-0123-7_11.

[8] M.L. Rocco, M. Soligo, L. Manni, L. Aloe, Nerve growth factor: early studies and recent clinical trials, CN 16 (2018) 1455–1465, https://doi.org/10.2174/1570159X16666180412092859.
[9] G. Alastra, L. Aloe, V.A. Baldassarro, L. Calzà, M. Cescatti, J.T. Duskey, M. L. Focarete, D. Giacomini, L. Giardino, V. Giraldi, L. Lorenzini, M. Moretti, I. Parmeggiani, M. Sannia, G. Tosi, Nerve growth factor biodelivery: a limiting step in moving toward extensive clinical application? Front. Neurosci. 15 (2021) 695592 https://doi.org/10.3389/fnins.2021.695592.
[10] B.L. Wise, M.F. Seidel, N.E. Lane, The evolution of nerve growth factor inhibition in clinical medicine, Nat. Rev. Rheuma 17 (2021) 34–46, https://doi.org/10.1038/s41584-020-00528-4.
[11] L.Y. Yung, P.H. Tso, E.H.T. Wu, J.C.H. Yu, N.Y. Ip, Y.H. Wong, Nerve growth factor-induced stimulation of p38 mitogen-activated protein kinase in PC12 cells is partially mediated via Gi/o proteins, Cell. Signal. 20 (2008) 1538–1544, https://doi.org/10.1016/j.cellsig.2008.04.007.
[12] A. Cuadrado, A.R. Nebreda, Mechanisms and functions of p38 MAPK signalling, Biochem. J. 429 (2010) 403–417, https://doi.org/10.1042/BJ20100323.
[13] B. Canovas, A.R. Nebreda, Diversity and versatility of p38 kinase signalling in health and disease, Nat. Rev. Mol. Cell Biol. 22 (2021) 346–366, https://doi.org/10.1038/s41580-020-00322-w.
[14] J. Xing, J.M. Kornhauser, Z. Xia, E.A. Thiele, M.E. Greenberg, Nerve growth factor activates extracellular signal-regulated kinase and p38 mitogen-activated protein kinase pathways to stimulate CREB serine 133 phosphorylation, Mol. Cell. Biol. 18 (1998) 1946–1955, https://doi.org/10.1128/MCB.18.4.1946.
[15] M. Uchiyama, M. Mihara, Determination of malonaldehyde precursor in tissues by thiobarbituric acid test, Anal. Biochem. 86 (1978) 271–278, https://doi.org/10.1016/0003-2697(78)90342-1.
[16] G.L. Ellman, A colorimetric method for determining low concentrations of mercaptans, Arch. Biochem. Biophys. 74 (1958) 443–450, https://doi.org/10.1016/0003-9861(58)90014-6.
[17] K.J. Livak, T.D. Schmittgen, Analysis of relative gene expression data using real-time quantitative PCR and the 2−ΔΔCT method, Methods 25 (2001) 402–408, https://doi.org/10.1006/meth.2001.1262.
[18] L. Chen, J. Min, F. Wang, Copper homeostasis and cuproptosis in health and disease, Sig Transduct. Target Ther. 7 (2022) 378, https://doi.org/10.1038/s41392-022-01229-y.
[19] Y. Li, Copper homeostasis: emerging target for cancer treatment, IUBMB Life 72 (2020) 1900–1908, https://doi.org/10.1002/iub.2341.
[20] M.-S. Tsai, P.-H. Lee, C.-K. Sun, T.-C. Chiu, Y.-C. Lin, I.-W. Chang, P.-H. Chen, Y.-H. Kao, Nerve growth factor upregulates sirtuin 1 expression in cholestasis: a potential therapeutic target, e426–e426, Exp. Mol. Med. 50 (2018), https://doi.org/10.1038/emm.2017.235.
[21] M.-S. Tsai, Y.-C. Lin, C.-K. Sun, S.-C. Huang, P.-H. Lee, Y.-H. Kao, Up-regulation of nerve growth factor in cholestatic livers and its hepatoprotective role against oxidative stress, PLoS One 9 (2014) e112113, https://doi.org/10.1371/journal.pone.0112113.
[22] M. Ceccanti, R. Coccurello, V. Carito, S. Ciafrè, G. Ferraguti, G. Giacovazzo, R. Mancinelli, P. Tirassa, G.N. Chaldakov, E. Pascale, M. Ceccanti, C. Codazzo, M. Fiore, Paternal alcohol exposure in mice alters brain NGF and BDNF and increases ethanol-elicited preference in male offspring: Paternal alcohol exposure, Addict. Biol. 21 (2016) 776–787, https://doi.org/10.1111/adb.12255.
[23] F. Oakley, N. Trim, C.M. Constandinou, W. Ye, A.M. Gray, G. Frantz, K. Hillan, T. Kendall, R.C. Benyon, D.A. Mann, J.P. Iredale, Hepatocytes express nerve growth factor during liver injury, Am. J. Pathol. 163 (2003) 1849–1858, https://doi.org/10.1016/S0002-9440(10)63544-4.
[24] C. Valdovinos-Flores, M.E. Gonsebatt, Nerve growth factor exhibits an antioxidant and an autocrine activity in mouse liver that is modulated by buthionine sulfoximine, arsenic, and acetaminophen, Free Radic. Res. 47 (2013) 404–412, https://doi.org/10.3109/10715762.2013.783210.
[25] S.S. Al-Rejaie, A.M. Aleisa, H.M. Abuohashish, M.Y. Parmar, M.S. Ola, A.A. Al-Hosaini, M.M. Ahmed, Naringenin neutralises oxidative stress and nerve growth factor discrepancy in experimental diabetic neuropathy, Neurol. Res. 37 (2015) 924–933, https://doi.org/10.1179/1743132815Y.0000000079.
[26] S. Gezginci-Oktayoglu, O. Sacan, R. Yanardag, A. Karatug, S. Bolkent, Exendin-4 improves hepatocyte injury by decreasing proliferation through blocking NGF/TrkA in diabetic mice, Peptides 32 (2011) 223–231, https://doi.org/10.1016/j.peptides.2010.10.025.
[27] J. Han, J. Wu, J. Silke, An overview of mammalian p38 mitogen-activated protein kinases, central regulators of cell stress and receptor signaling, F1000Res 9 (2020) 653, https://doi.org/10.12688/f1000research.22092.1.
[28] H. Liu, H. Guo, H. Deng, H. Cui, J. Fang, Z. Zuo, J. Deng, Y. Li, X. Wang, L. Zhao, Copper induces hepatic inflammatory responses by activation of MAPKs and NF-κB signalling pathways in the mouse, Ecotoxicol. Environ. Saf. 201 (2020) 110806, https://doi.org/10.1016/j.ecoenv.2020.110806.
[29] H. Cui, C. Shao, Q. Liu, W. Yu, J. Fang, W. Yu, A. Ali, K. Ding, Heparanase enhances nerve-growth-factor-induced PC12 cell neuritogenesis via the p38 MAPK pathway, Biochem. J. 440 (2011) 273–282, https://doi.org/10.1042/BJ20110167.
[30] R.E. Mufti, K. Sarker, Y. Jin, S. Fu, J.L. Rosales, K.-Y. Lee, Thrombin enhances NGF-mediated neurite extension via increased and sustained activation of p44/42 MAPK and p38 MAPK, PLoS One 9 (2014) e103530, https://doi.org/10.1371/journal.pone.0103530.
[31] B. Gao, W. Sun, X. Meng, D. Xue, W. Zhang, Screening of differentially expressed protein kinases in bone marrow endothelial cells and the protective effects of the p38a inhibitor SB203580 on bone marrow in liver fibrosis, Mol. Med. Rep. 14 (2016) 4629–4637, https://doi.org/10.3892/mmr.2016.5837.
[32] J.-T. Hsu, P.-H. Le, C.-J. Lin, T.-H. Chen, C.-J. Kuo, K.-C. Chiang, T.-S. Yeh, Mechanism of salutary effects of melatonin-mediated liver protection after trauma-hemorrhage: p38 MAPK-dependent iNOS/HIF-1α pathway, Am. J. Physiol. Gastrointest. Liver Physiol. 312 (2017) G427–G433, https://doi.org/10.1152/ajpgi.00440.2016.
[33] H. Zhang, I. Ozaki, T. Mizuta, S. Matsuhashi, T. Yoshimura, A. Hisatomi, J. Tadano, T. Sakai, K. Yamamoto, β1-integrin protects hepatoma cells from chemotherapy induced apoptosis via a mitogen-activated protein kinase dependent pathway, Cancer 95 (2002) 896–906, https://doi.org/10.1002/cncr.10751.
[34] J.C. Lee, J.T. Laydon, P.C. McDonnell, T.F. Gallagher, S. Kumar, D. Green, D. McNulty, M.J. Blumenthal, J.R. Keys, S.W. Land Vatter, J.E. Strickler, M. M. McLaughlin, I.R. Siemens, S.M. Fisher, G.P. Livi, J.R. White, J.L. Adams, P. R. Young, A protein kinase involved in the regulation of inflammatory cytokine biosynthesis, Nature 372 (1994) 739–746, https://doi.org/10.1038/372739a0.
[35] J.C. Lee, S. Kumar, D.E. Griswold, D.C. Underwood, B.J. Votta, J.L. Adams, Inhibition of p38 MAP kinase as a therapeutic strategy, Immunopharmacology 47 (2000) 185–201, https://doi.org/10.1016/S0162-3109(00)00206-X.
[36] S. Banerjee Mustafi, P.K. Chakraborty, R.S. Dey, S. Raha, Heat stress upregulates chaperone heat shock protein 70 and antioxidant manganese superoxide dismutase through reactive oxygen species (ROS), p38MAPK, and Akt, Cell Stress Chaperon.. 14 (2009) 579–589, https://doi.org/10.1007/s12192-009-0109-x.
[37] L. He, T. He, S. Farrar, L. Ji, T. Liu, X. Ma, Antioxidants maintain cellular redox homeostasis by elimination of reactive oxygen species, Cell Physiol. Biochem. 44 (2017) 532–553, https://doi.org/10.1159/000485089.
[38] Y. Son, S. Kim, H.-T. Chung, H.-O. Pae, Reactive oxygen species in the activation of MAP kinases, in: Methods in Enzymology, Elsevier, 2013, pp. 27–48, https://doi.org/10.1016/B978-0-12-405881-1.00002-1.
[39] M.D. Mattie, M.K. McElwee, J.H. Freedman, Mechanism of copper-activated transcription: activation of AP-1, and the JNK/SAPK and p38 signal transduction pathways, J. Mol. Biol. 383 (2008) 1008–1018, https://doi.org/10.1016/j.jmb.2008.08.080.
[40] F. Benedetti, S. Davinelli, S. Krishnan, R.C. Gallo, G. Scapagnini, D. Zella, S. Curreli, Sulfur compounds block MCP-1 production by Mycoplasma fermentans-infected macrophages through NF-κB inhibition, J. Transl. Med. 12 (2014) 145, https://doi.org/10.1186/1479-5876-12-145.
[41] J.A. DiDonato, F. Mercurio, M. Karin, NF-κB and the link between inflammation and cancer, Immunol. Rev. 246 (2012) 379–400, https://doi.org/10.1111/j.1600-065X.2012.01099.x.
[42] H. Qiao, J.M. May, Macrophage differentiation increases expression of the ascorbate transporter (SVCT2), Free Radic. Biol. Med. 46 (2009) 1221–1232, https://doi.org/10.1016/j.freeradbiomed.2009.02.004.
[43] J. Patwa, S.J.S. Flora, MiADMSA abrogates chronic copper-induced hepatic and immunological changes in Sprague Dawley rats, Food Chem. Toxicol. 145 (2020) 111692, https://doi.org/10.1016/j.fct.2020.111692.
[44] G. Minnone, F. De Benedetti, L. Bracci-Laudiero, NGF and its receptors in the regulation of inflammatory response, IJMS 18 (2017) 1028, https://doi.org/10.3390/ijms18051028.
[45] G.P. Sreekanth, A. Chuncharunee, A. Sirimontaporn, J. Panaampon, S. Noisakran, P. Yenchitsomanus, T. Limjindaporn, SB203580 modulates p38 MAPK signaling and dengue virus-induced liver injury by reducing MAPKAPK2, HSP27, and ATF2 phosphorylation, PLoS ONE 11 (2016) e0149486, https://doi.org/10.1371/journal.pone.0149486.
[46] Z. Jian, H. Guo, H. Liu, H. Cui, J. Fang, Z. Zuo, J. Deng, Y. Li, X. Wang, L. Zhao, Oxidative stress, apoptosis and inflammatory responses involved in copper-induced pulmonary toxicity in mice, Aging 12 (2020) 16867–16886, https://doi.org/10.18632/aging.103585.
[47] M.M.S. AL-Musawi, H. Al-Shmgani, G.A. Al-Bairuty, Histopathological and biochemical comparative study of copper oxide nanoparticles and copper sulphate toxicity in male albino mice reproductive system, Int. J. Biomater. 2022 (2022) 1–12, https://doi.org/10.1155/2022/4877637.
[48] S. Santos, A.M. Silva, M. Matos, S.M. Monteiro, A.R. Álvaro, Copper induced apoptosis in Caco-2 and Hep-G2 cells: expression of caspases 3, 8 and 9, AIF and p53, Comp. Biochem. Physiol. Part C Toxicol. Pharmacol. 185–186 (2016) 138–146, https://doi.org/10.1016/j.cbpc.2016.03.010.
[49] W. Zhong, H. Zhu, F. Sheng, Y. Tian, J. Zhou, Y. Chen, S. Li, J. Lin, Activation of the MAPK11/12/13/14 (p38 MAPK) pathway regulates the transcription of autophagy genes in response to oxidative stress induced by a novel copper complex in HeLa cells, Autophagy 10 (2014) 1285–1300, https://doi.org/10.4161/auto.28789.
[50] Q. Bai, M. Zou, J. Zhang, Y. Tian, F. Wu, B. Gao, F. Piao, NGF mediates protection of mesenchymal stem cells-conditioned medium against 2,5-hexanedione-induced apoptosis of VSC4.1 cells via Akt/Bad pathway, Mol. Cell Biochem. 469 (2020) 53–64, https://doi.org/10.1007/s11010-020-03727-5.
[51] D. Liu, H. Wang, Y. Zhang, Z. Zhang, Protective effects of chlorogenic acid on cerebral ischemia/reperfusion injury rats by regulating oxidative stress-related Nrf2 pathway, DDDT 14 (2020) 51–60, https://doi.org/10.2147/DDDT.S228751.
[52] Q. Wang, R. Chen, C. Zhang, Inam-u-llah, F. Piao, X. Shi, NGF protects bone marrow mesenchymal stem cells against 2,5-hexanedione-induced apoptosis in vitro via Akt/Bad signal pathway, Mol. Cell Biochem. 457 (2019) 133–143, https://doi.org/10.1007/s11010-019-03518-7.